Evidence for weak link and anisotropy limitations on the transport critical current in bulk polycrystalline $Y_1Ba_2Cu_3O_x$

J. W. Ekin
Electromagnetic Technology Division, National Bureau of Standards, Boulder, Colorado 80303

A. I. Braginski, A. J. Panson, and M. A. Janocko
Westinghouse Research & Development Center, Pittsburgh, Pennsylvania 15235

D. W. Capone II, N. J. Zaluzec, B. Flandermeyer, and O. F. de Lima
Argonne National Laboratory, Argonne, Illinois 60439

M. Hong, J. Kwo, and S. H. Liou
AT&T Bell Laboratories, Murray Hill, New Jersey 07974

(Received 29 June 1987; accepted for publication 1 September 1987)

Measurements of the transport critical-current density (J_c), magnetization J_c, and magnetoresistance in a number of bulk sintered samples of $Y_1Ba_2Cu_3O_x$ from several different laboratories indicate that the transport J_c is limited by weak-link regions between high J_c regions. The weak-link J_c has a Josephson character, decreasing by two orders of magnitude as the magnetic field is increased from 0.1 to 10 mT at 77 K. An examination of the grain-boundary region in $Y_1Ba_2Cu_3O_x$ shows no observable impurities or second phases to the scale of the [001] lattice planes (~ 12 Å). The effect of intrinsic conduction anisotropy is discussed. A current-transfer model is proposed in which weak conduction along the c axis plays a role in limiting J_c at grain boundaries. Orienting the grains in the powder state during processing may result in enhanced transport J_c in bulk conductors.

I. INTRODUCTION

Following the discovery of high-temperature superconductivity by Bednorz and Müller in metallic oxides,[1] a number of similar materials have been observed to have high transition temperatures, most notably the La-Sr-Cu-O system[2–5] with transition temperatures in the range 30–40 K, and the Y-Ba-Cu-O system[6] with transition temperatures above 90 K. Although the critical temperature T_c of these materials is high, their range of application will be determined by their ability to carry current. Most applications require high-current densities, usually more than 10^4–10^5 A/cm^2. Bulk applications usually further require high-current capacity and high J_c in the presence of a significant magnetic field (1–10 T). In *zero applied magnetic field*, the highest J_c reported[7] at 77 K for bulk polycrystalline $Y_1Ba_2Cu_3O_x$ material is about 10^3 A/cm^2, with J_c values in the range of 200 A/cm^2 being more usual.[8] This value of J_c is significantly lower than that needed for most bulk applications. In a magnetic field, J_c is much lower.

Although values of J_c are commonly calculated from magnetization data, very little data are available on directly measured values of the transport J_c for $Y_1Ba_2Cu_3O_x$ in magnetic-fields. The first measurements of the magnetic-field dependence of the transport J_c in $Y_1Ba_2Cu_3O_x$ were recently reported.[8,9]

This paper is based on those data along with additional data on transport J_c, magnetization J_c, strain effect on J_c, magnetoresistance, and transmission electron microscopy of the grain-boundary region in bulk polycrystalline $Y_1Ba_2Cu_3O_x$.

A number of bulk sintered polycrystalline samples from several different laboratories were tested. The data show three characteristics which were common to all samples: (1) For $T < T_c$ the transition of the resistance of the material from the normal-state value to zero occurs gradually over a very wide magnetic-field range. (2) The transport J_c drops sharply by two orders of magnitude between 0.1 and 10 mT. (3) The transport J_c is about two orders of magnitude lower than the J_c calculated from magnetization data under the assumption of a homogeneous current distribution.

These general characteristics are interpreted as evidence that the transport J_c in bulk polycrystalline $Y_1Ba_2Cu_3O_x$ is dominated by weak-link regions separating high J_c regions in the material.[8,10,11] Possible causes of the weak-link phenomenon are considered, including impurities and compositional variations at the grain boundaries, and intrinsic anisotropy of the superconducting properties. Microscopic examination of the grain-boundary region of $Y_1Ba_2Cu_3O_x$ by transmission electron microscopy (TEM) shows no observable impurities or second phase at the grain boundaries to the scale of the [001] lattice planes (~ 12 Å). X-ray energy-dispersive spectroscopy (XEDS), and electron-energy-loss spectroscopy (EELS) also show no changes in composition at the grain boundary, but to a coarser scale of about 200 Å. The microscopy data showing the mismatch of the Cu-O planes at the grain boundaries, plus the intrinsic anisotropy of J_c observed in single crystals,[12] indicates that one of the factors limiting J_c in polycrystalline material may be intrinsic conduction anisotropy. The process of current redistribution among the highly conducting Cu-O planes at grain boundaries will be limited by the intrinsic weak conduction perpendicular to the Cu-O planes. This suggests that orienting the grains in bulk materials would have the potential to realize an enhanced J_c, and may account for some of the difference in J_c between polycrystalline samples and epitaxial $Y_1Ba_2Cu_3O_x$ films.[13] Some general guidelines for tech-

 0021-8979/87/244821-08$02.40

niques to accomplish this in bulk samples are outlined in Ref. 14.

II. EXPERIMENT

Bulk sintered samples of $Y_1Ba_2Cu_3O_x$ (where $x \lesssim 7$) from three different laboratories were tested.[9,15,16] Preparation details on specific samples are given in Table I. Typically the samples were made from powders of CuO, Y_2O_3, and $BaCO_3$ which were weighed after drying and then reacted at high temperature, usually in an oxygen atmosphere. The materials were homogenized by repeated grinding, mixing, and heating in flowing oxygen. This was followed by cold pressing the powder into final form and sintering the sample at high temperature in flowing oxygen. The samples were then cooled and soaked in flowing oxygen at temperatures between about 400 and 500 °C.

As noted in Table I, grain sizes ranged from 10 to 50 μm, and the distribution of grain sizes was quite wide. Samples were about 75%–95% dense, as listed in Table I. A scanning electron micrograph of the surface of sample 4 is shown in Fig. 1.

All samples were in the form of bars, 1–3 cm long, with a cross-sectional area of about 2 mm^2. The samples were tested using a four-terminal technique in magnetic fields ranging from 0.1 mT to 19 T.

Considerable care was taken to ensure that the results were not affected by heating at the current contacts. A lower limit on the contact heating level needed to drive the sample normal in liquid nitrogen was determined from a sample with relatively resistive current contacts. All data obtained at 77 K which are reported here were obtained on samples where the contact heating was at least 100 times less than this lower limit.

J_c measurements were also made at temperatures below 77 K. These data were obtained using a 13.5-T superconducting magnet and a variable-temperature gas-flow cryostat. Temperature control was maintained using a capacitance thermometer with a precision better than 0.1 K. Data are reported at these lower temperatures only for currents low enough that the heating levels were ten times less than the power level where the *V-I* curves showed heating effects as evidenced by irreversibility.

III. RESULTS

A. *V-I* characteristics and magnetoresistance *R(H)*

Figures 2 and 3 show the voltage versus current (*V-I*) characteristics for two of the samples measured at fields from 1 mT to 19 T at 77 K in liquid nitrogen. The striking feature about these characteristics is that the voltage did not rise abruptly to the normal resistance value as current was raised above the critical current I_c. At current levels well above the critical current (indicated by arrows along the abscissa) the *V-I* characteristics were nearly linear and had a slope that was much less than the normal resistance of the sample at T_c. As magnetic field was increased, the slope increased toward the normal-resistance value. We estimate on the basis of the high-field data that fields over 30 T are required to completely reach the normal-resistance value, i.e., suppress all superconductivity. In contrast, very low fields, only a few tesla, were required to suppress the transport I_c as noted by the arrows along the abscissa in Figs. 2 and 3.

Thus, there is a very wide range of magnetic field over which the material transforms from the superconducting to the normal state. Figure 4 shows the magnetic-field dependence of the resistance at 77 K of two samples measured *at current levels much greater than* I_c (that is, where I_c is exceeded and the *V-I* characteristic is linear as shown in Figs. 2 and 3). At a magnetic field of 20 T, the resistance is only about 40% of the normal resistance, R_n, measured in low magnetic field just above T_c. Figure 4 also shows that the decrease in resistance levels off at low field to a value of about 10% to 13% of R_n.

B. Transport critical-current density versus magnet field, $J_c(H)$

Figure 5 shows a typical trace of the low voltage region of the *V-I* characteristics below I_c. This curve was taken in zero applied magnetic field, but in the presence of the earth's field of about 0.5×10^{-4} T. The *V-I* curve was reversible.

TABLE I. Sample characteristics.

	Samples 2,4	Sample 5	Samples 1,3
Heat treatment	Fire and premix twice Final treatment: 940 °C for 16 h in O_2 700 °C for 16 h in O_2 slow cool in O_2	Calcine at 950 °C 3 h to 400 °C 5 h to 975 °C hold for 5 h slow cool in O_2	Grind and sinter three times 950 °C for 10 h in O_2 slow cool in O_2
Average grain size	10 μm	20–50 μm	10 μm
Grain size distribution		wide	3–20 μm
Density	75%	90%–95%	75%
Superconductor cross-sectional area	Sample 2: 1.98 mm^2 Sample 4: 1.42 mm^2	1.77 mm^2	Sample 1: 0.74 mm^2 Sample 3: 2.11 mm^2
$\rho(T_c)$	Sample 2: 595 $\mu\Omega$ cm Sample 4: 344 $\mu\Omega$ cm	1088 $\mu\Omega$ cm	Sample 1: 254 $\mu\Omega$ cm Sample 3: 317 $\mu\Omega$ cm

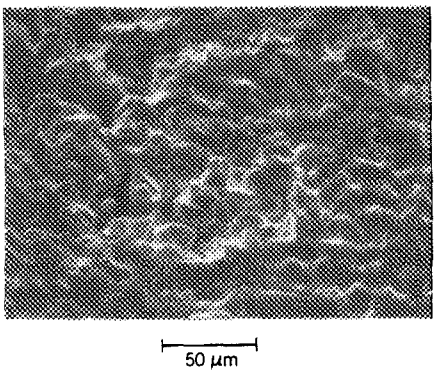

FIG. 1. Scanning electron micrograph of surface of sample 4 showing granular structure.

The data show that the voltage below the critical current is zero within experimental accuracy ($\pm$ 50 nV).

As magnetic field is increased, the onset of the upward curvature in the *V-I* curve is shifted toward zero, as shown in Fig. 6. The onset reached zero current at a magnetic field of about 2–5 T. At higher fields the sample appears to have finite resistance at zero current. The measurement accuracy is limited at low-resistance levels because of the very low current, thus it is difficult to examine this region of the *V-I* curve. However, there is a clear nonlinearity or offset in the *V-I* characteristic even in fields as high as 10 T. Thus, there is some remnant of superconductivity evidenced by the transport current in fields of at least 10 T, although the current and resistance levels are far from any practical value.

The critical-current density measured in seven samples in the earth's magnetic field ranged from a low of about 10 A/cm^2 to a high of about 200 A/cm^2. Thus, the transport critical-current densities were generally low and variable. No correlation between the critical current and the external-lead contact resistance was observed, confirming that contact heating at the current connections was not the cause of the low J_c values. Also, as noted above, data are presented only on samples for which the contact heating was at least two orders of magnitude below the minimum contact heating level needed to drive the superconductor normal.

When magnetic field is applied perpendicular to the direction of transport current, J_c is suppressed significantly below the zero-field value. Figure 7 shows the magnetic-field dependence of J_c in two samples. The critical-current density for both samples decreased sharply by more than two orders of magnitude as magnetic field increased from 0.1 to 10 mT. The decrease in J_c with magnetic field was less rapid above 1 T, but in this region the J_c-vs-field plot is strongly dependent on the criterion used to determine J_c. (The higher J_c region below 1 T is not greatly affected by this criterion, however.) Two criteria are shown in Fig. 7. The solid curves correspond to an electric-field criterion of 1 μV/mm, along with a correction for current carried by the sample when it is in the normal state. The dashed curves are for a resistivity criterion of 1 $\mu\Omega$ cm. Only very coarse resistivity criteria could be applied to the data in the high-field region where the critical current is extremely low because of the limits on electric-field detection in such short samples. (At very low fields where J_c is much higher, the resistivity criteria can be correspondingly more sensitive.) Regardless of which criterion is used, the data show that the effective upper critical field for transport J_c is significantly less than 10 T. This is much less than the estimated 30-T field needed to completely suppress all superconductivity (i.e., where the resistance approaches the normal-state value).

The effect of stress on the critical current of samples 3, 4, and 5 was also measured at very low tensile strains up to about 0.05%. Higher strains caused the samples to fracture. No significant effect was observed, but, on the other hand, no measurable effect was expected at this low strain level. In Nb_3Sn, for example, where the critical current is relatively sensitive to strain, the effect of 0.05% strain at low fields is to degrade the critical current by only 0.3%.[17]

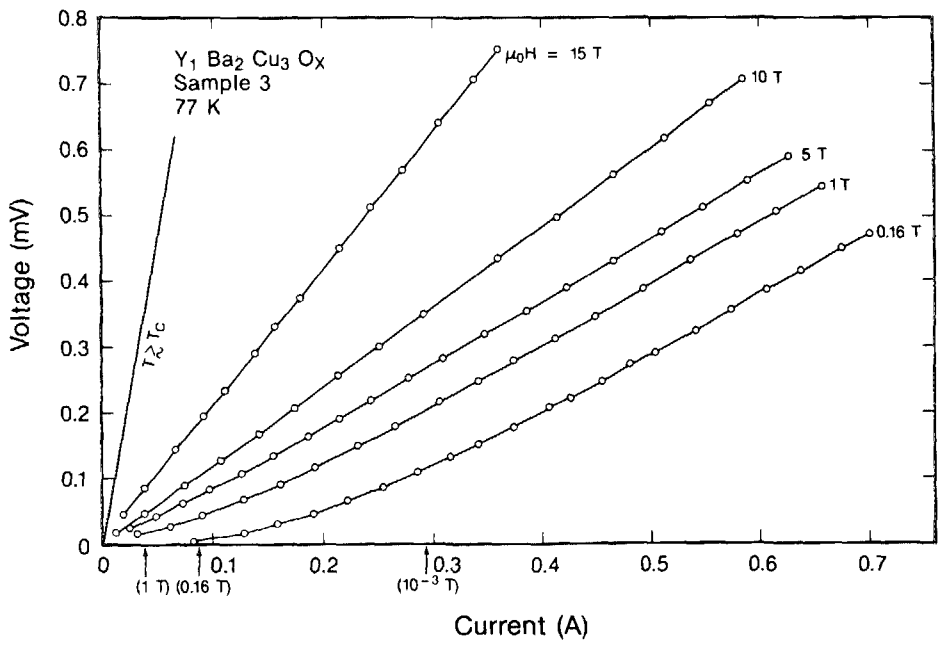

FIG. 2. Voltage vs current characteristics for sample 3 in transverse magnetic fields in liquid nitrogen at 77 K. At currents well above the critical current (indicated by arrows along the abscissa) the *V-I* curves were nearly linear. High magnetic fields are required to increase the slope to the normal-resistance value at T_c, but the transport J_c is suppressed by very low fields.

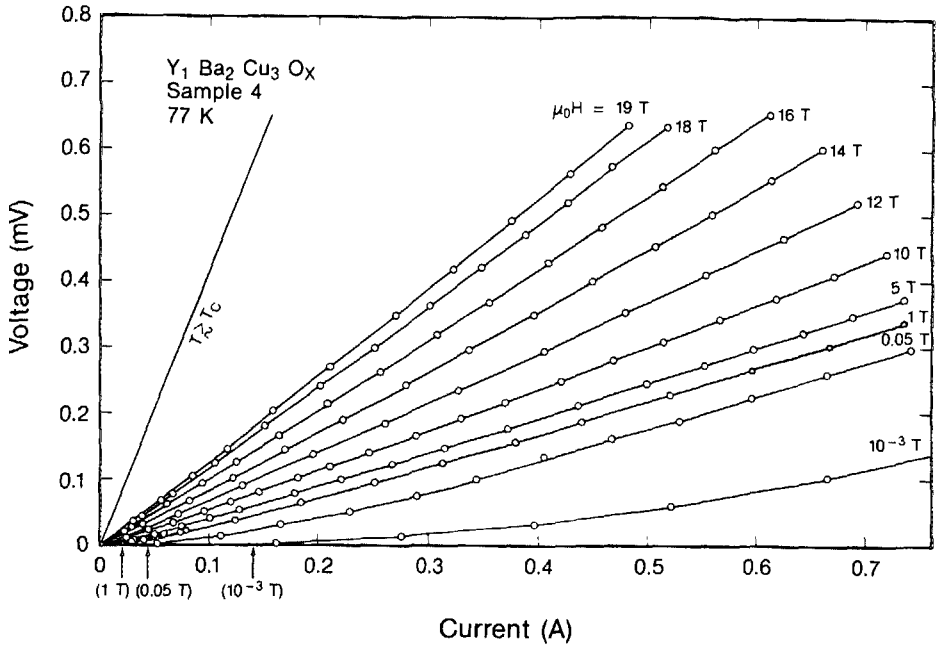

FIG. 3. Voltage vs current dependence for sample 4 in transverse magnetic fields showing results similar to Fig. 2 and the generality of the shape of the transport characteristics for different samples (after Ref. 8).

The characteristics reported here appear to be general among different samples made by different laboratories. All samples showed the same features of a linear V-I curve above I_c, a high field required to totally suppress all superconductivity, and a low field required to suppress the critical current.

Data on J_c versus magnetic field at temperatures below 77 K are presented in Fig. 8. J_c was determined using an electric-field criterion of 0.1 μV/mm. The data labeled "$H = 0$" were taken in the residual field of the superconducting magnet (~ 1 mT). This sample has a J_c of 233 A/cm^2 in the earth's field and 77 K. The temperature dependence of J_c near T_c is shown in Fig. 9.

C. Magnetization J_c versus transport J_c

These values for the *transport* J_c appear significantly lower than values of J_c calculated from *magnetization* measurements assuming that the induced current distribution is homogeneous. J_c has been calculated at fields above 0.5 T from magnetization data of Panson *et al.*[15] at 77 K on a material fabricated in the same way as sample 3 in Fig. 7. Values of magnetization J_c are shown as a dotted line in Fig. 7 at magnetic field between 0.5 and 6 T. A comparison with the transport J_c shown in Fig. 7 for sample 3 indicates that the magnetization J_c is about two orders of magnitude higher than the transport J_c over the same magnetic-field range.

IV. EVIDENCE FOR WEAK-LINK COUPLING

These results indicate that the ranges of values of both the upper critical field and J_c in polycrystalline $Y_1Ba_2Cu_3O_x$ are very broad. More specifically, the data are consistent with a model in which the transport J_c is dominated by weak-link regions having very low J_c, separating high J_c regions in the material. The evidence offered by these data for such a hypothesis is described in this section.

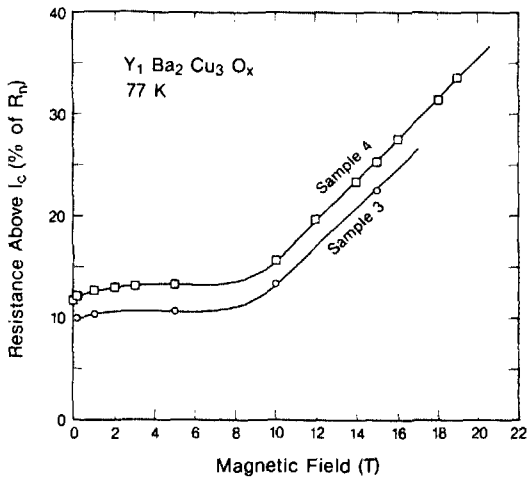

FIG. 4. Magnetic-field dependence of the resistance of $Y_1Ba_2Cu_3O_x$ above I_c. The resistance is shown as a percentage of the normal-state resistance, R_n, measured at T_c in low magnetic field.

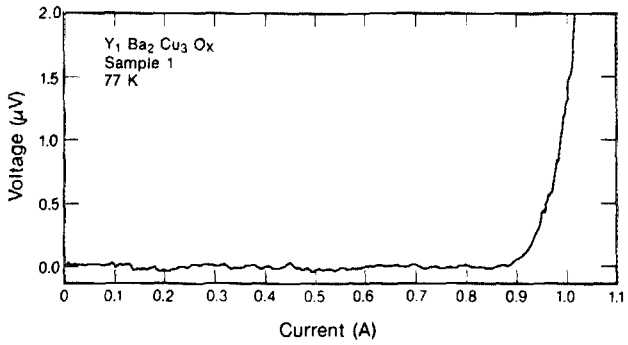

FIG. 5. Voltage vs current characteristic in earth's magnetic field (~ 0.05 mT) showing the absence of detectable voltage below the critical current (after Ref. 8).

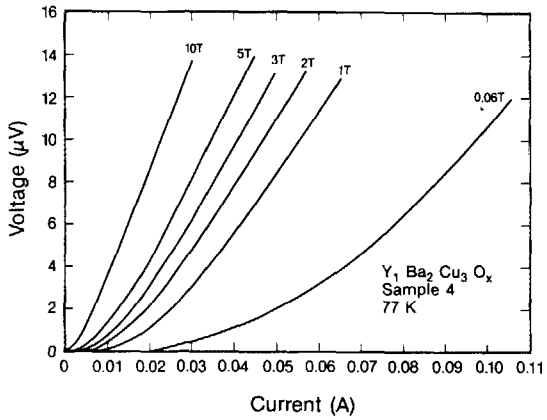

FIG. 6. Voltage vs current characteristics in applied transverse magnetic fields up to 10 T.

A. *R(H)*

The very wide magnetic-field range over which the resistivity of the material increases from zero to the normal-state value is indicative of an inhomogeneous material with a wide range of H_{c2}. Figure 4 shows that at very low magnetic fields the resistance is nearly constant. As magnetic field is increased, there is a break in the curve at about 3 T and the resistance starts to increase toward the normal-state value. We speculate that this nearly constant low-field resistance is a regime wherein the transport current has driven the weak-link region normal, but the applied field is much less than H_{c2} for the high J_c regions. Assuming this is true, we find for these two samples that the weak-link region contributes a resistance equal to about 10%–13% of the normal-state resistance at T_c.

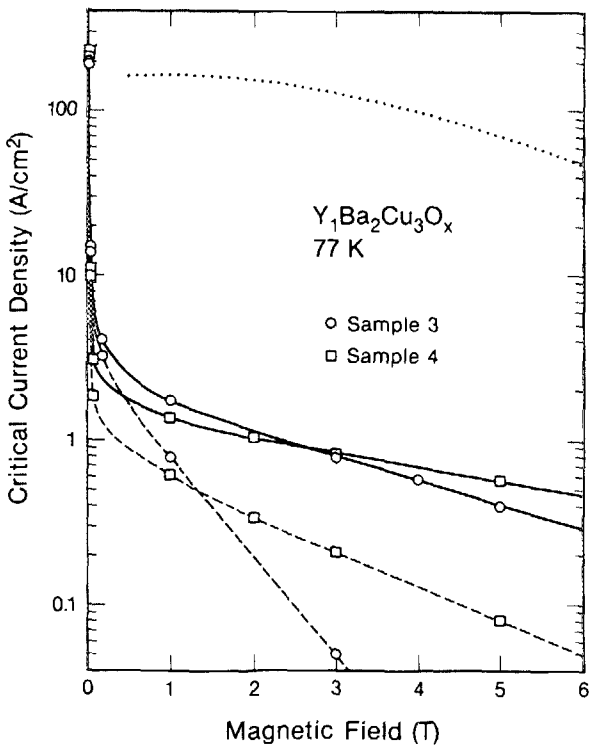

FIG. 7. Transport critical-current density J_c vs perpendicular magnetic field for polycrystalline $Y_1Ba_2Cu_3O_x$ samples at 77 K. The solid line corresponds to an electric-field criterion of 1 μV/mm; the dashed line corresponds to a resistivity criterion of 1 $\mu\Omega$ cm; the dotted line indicates the magnetization J_c measured in a sample similar to sample 3. The two lowest-field points were taken at 0.05 and 1 mT. There is a very sharp decrease in J_c in this low-field regime.

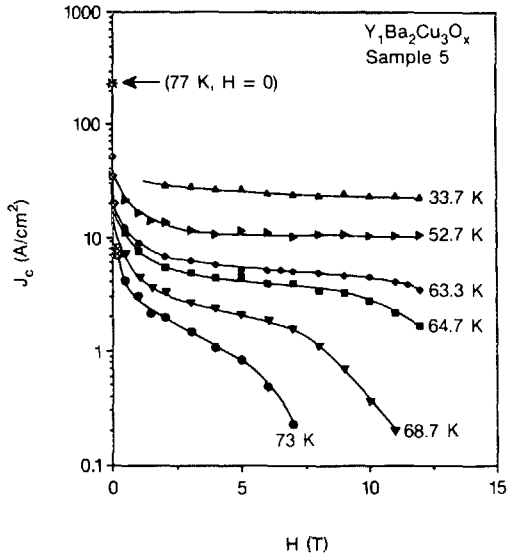

FIG. 8. Transport J_c vs magnetic field at temperatures below 77 K.

Under this interpretation, the constant resistance region of the $R(H)$ curve is a result of high measuring current and should disappear at sufficiently low currents. Thus, care should be used in focusing on this part of the R-vs-H curves to determine at what field the resistance reaches zero, since we suspect such results[11,18] are highly dependent on measuring current.

At higher fields around 8 T, where the $R(H)$ curve starts to turn upward, the magnetic field (rather than measuring current) starts to suppress superconductivity in the high J_c regions of the material. Some idea of the minimum H_{c2} at 77 K can be obtained by extrapolating the high-field characteristic in Fig. 4 to zero resistance. A straight line extrapolation reaches zero at about 3 T. This would indicate that the minimum value of the range of H_{c2} at 77 K is quite low, on the order of 3–8 T. This is consistent with the field range where the onset of resistance at zero current is ob-

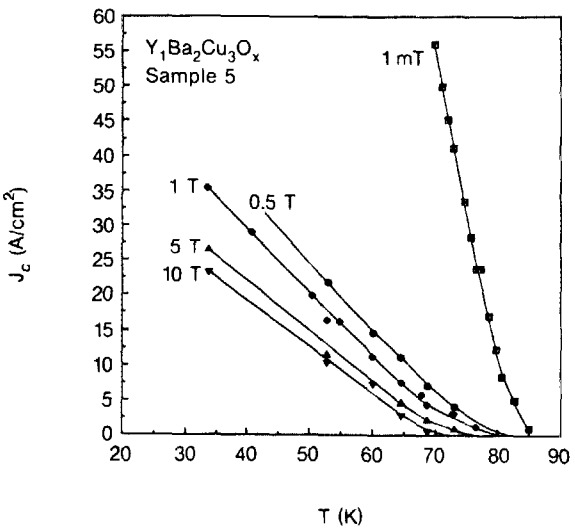

FIG. 9. Transport critical-current density J_c vs temperature for several values of applied magnetic field.

served in the critical-current curves of Fig. 6. The upper limit of the range of H_{c2} is much greater than 20 T, as indicated by the fact that the resistance reaches only 40% of the normal-state value at 20 T.

Thus, the data can be interpreted as evidence for a broad range of H_{c2} at 77 K extending from a minimum value of about 3 T to a maximum value much greater than 20 T. Such an interpretation is supported by recent data[12] showing anisotropic H_{c2} in single crystals of $Y_1Ba_2Cu_3O_x$. Recent calculations[18,19] show that the shape of the high-field portion of the $R(H)$ curve can be explained at least in part by an anisotropic H_{c2} and percolation paths through randomly oriented crystallites. In addition to H_{c2} anisotropy, conduction anisotropy (discussed below) may also be a contributing factor in interpreting these $R(H)$ data.

B. $J_c(H)$

The magnetic-field dependence of J_c is consistent with a picture in which the transport J_c is dominated by weak-link regions having very low J_c that separate high J_c regions within the material. In such a situation, the low J_c regions would dominate the transport J_c. The J_c decreases by two orders of magnitude between 0.1 and 10 mT. This rapid decrease in J_c at very low fields is indicative of Josephson weak-link currents, which are suppressed by very low magnetic fields. (We are using "Josephson weak-link" as a generic term and do not mean to differentiate between SIS, SNS, or SS'S weak-link conduction.)

C. Transport J_c versus magnetization J_c

The concept of low J_c regions connecting high J_c regions is further supported by the large (two orders of magnitude) difference between J_c measured directly from transport currents and J_c calculated from magnetization data using the Bean model.[20] If weak-link regions were present, they would completely dominate the transport J_c, but only partially affect the magnetization J_c. This is easy to see in the extreme case where the high J_c regions are completely decoupled by the weak regions. In such case, the transport J_c would be zero, but circulating supercurrents within the high J_c regions would still give a finite magnetization and, hence, a finite magnetization J_c. Values of J_c calculated using the Bean model are applicable only to homogeneous superconductor materials, not highly heterogeneous materials such as these. Thus, the large difference observed between the magnetization J_c and the transport J_c is evidence for high and low J_c regions with the weak region dominating the transport J_c. This interpretation is also consistent with observations by magnetic susceptibility[21] of two superconducting components in Y-Ba-Cu-O.

The spatial extent of the weak-link region is uncertain. Since the material is granular, inhomogeneities in the structure might occur on a scale the size of an individual grain. An upper limit on the size can be obtained from observations such as those reported in Ref. 10 where hysteresis of the magnetization ΔM is measured in a bulk sintered sample, and then the sample is powdered to near grain size and magnetization remeasured. There is not much change in the measured magnetization. We see typically $\Delta M_{\text{bulk}}/\Delta M_{\text{powder}} = 2$–5. This suggests that the high J_c regions occupy a region no larger than a grain. On the other hand, scanning tunneling data[22] on single-crystal samples suggest that there may be "granularity" within each grain. That is, the tunneling I-V traces at low bias show a linear conductance indicative of Coulomb gaps brought about by domains on a scale less than $\frac{1}{10}$ the grain size. Thus, the size scale of the heterogeneity is uncertain.

V. ROLE OF CONDUCTION ANISOTROPY

In this section we consider some possible sources of the weak-link behavior in $Y_1Ba_2Cu_3O_x$. The evidence is based on microscopy data of the grain-boundary regions in $Y_1Ba_2Cu_3O_x$ as well as recent data on epitaxial films and single-crystal $Y_1Ba_2Cu_3O_x$ samples.

An obvious possibility is impurities or second-phase material at the grain boundaries. A transmission electron micrograph (TEM) lattice image of a grain-boundary region in bulk polycrystalline $Y_1Ba_2Cu_3O_x$ is shown in Fig. 10. In this technique the diffraction conditions in the microscope are set up to image the [001] planes (parallel to the Cu-O planes) in adjacent $Y_1Ba_2Cu_3O_x$ grains. Hence, the c axis of the orthorhombic structure is normal to the observed fringes. In all cases where grain boundaries are observed between 1:2:3 crystalline regions of the materials, clean grain boundaries such as shown in Fig. 10(b) are observed. The lattice image shows no observable impurities or second phases at the grain boundaries to the scale of the [001] lattice plane ($\sim$12 Å). X-ray energy-dispersive spectroscopy (XEDS) and electron-energy-loss spectroscopy (EELS) have confirmed that each grain is nominally 1:2:3 ($Y_1Ba_2Cu_3O_x$) in metal composition to a resolution of about 200 Å. These results are also consistent with x-ray analysis on the La-Sr-Cu-O system where no change in composition near the grain boundary was observed.[23] This implies that if impurities, second phases, or compositional variations are a factor at the grain boundaries, they would have to be acting on a scale finer than that observed. A significant effect on such a fine scale cannot be ruled out, however,

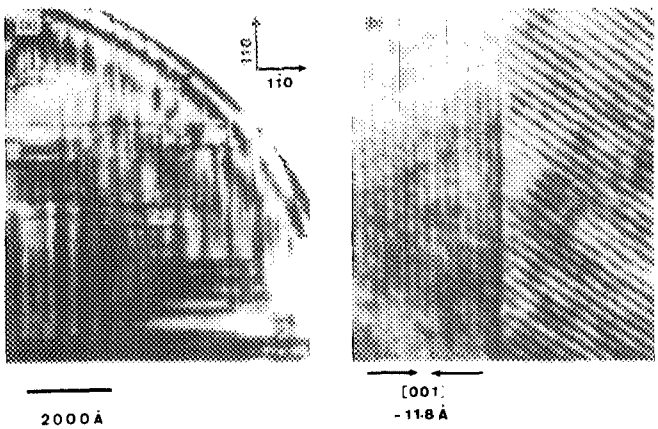

FIG. 10. (a) Low magnification TEM micrograph of twin boundaries within a grain of $Y_1Ba_2Cu_3O_x$. (b) High-resolution TEM of the boundary region between grains obtained using a lattice imaging technique. There is a misalignment of the Cu-O atomic planes at the grain boundary in polycrystalline $Y_1Ba_2Cu_3O_x$.

because of the very small coherence length in these materials. Higher-resolution analysis are needed, particularly of possible compositional variations near grain boundaries.

There are regions of all samples ($<20\%$ by volume) which consist of either amorphous or fine-grained (~ 20 Å) polycrystalline material possessing distinctly different compositions than 1:2:3. However, the amount of this type of material is insufficient to produce a lack of percolation between the 1:2:3 crystalline materials.

We now consider the inherent anisotropy of the superconducting properties of the $Y_1Ba_2Cu_3O_x$ crystal structure as a possible mechanism contributing to the low J_c in polycrystalline $Y_1Ba_2Cu_3O_x$. Recent data[12] on single-crystal samples of $Y_1Ba_2Cu_3O_x$ show that there is a strong anisotropy in the magnetization J_c within the $Y_1Ba_2Cu_3O_x$ crystal structure, with conduction in the plane of the Cu-O chains being higher than in the direction perpendicular to these planes. For example, at 40 K in a field of 1 T, the J_c anisotropy between conduction parallel and perpendicular to the Cu-O planes in one sample was more than 500 and increased rapidly with field. Other samples were reported to show anisotropy several times larger.[12] (This is a lower bound on the J_c anisotropy, since the anisotropy was reported to decrease more than an order of magnitude at 2 T for a 5° misalignment of the crystal.) The upper critical field has been observed to have significant anisotropy as well.[12,24]

The magnetic-field dependence of J_c obtained from magnetization data[12] in single crystals also shows a much sharper fall off for J_c perpendicular to the Cu-O planes (the c-axis direction) than parallel, decreasing more than two orders of magnitude between 0 and 1 T at 40 K. At 77 K, no single-crystal data were available, but judging from the trend, we expect the decrease with magnetic field to be greater at higher temperatures. These single-crystal results indicate that at least part of the sharp decrease of J_c with magnetic field in bulk samples at higher temperatures may arise from the intrinsic properties of weak conduction in the c-axis direction.

The steep magnetic-field dependence indicates that conduction along the c axis may have a Josephson weak-link character[25] with a steep magnetic-field dependence at low field. Recent band-structure calculations[26] indicate a two-dimensional Fermi surface with a charge deficit in the vicinity of the rare-earth planes, so there is some physical basis for expecting such a weak-link conduction character in the c-axis direction. Alternatively, weak flux pinning for current conduction in this direction may also be a factor contributing to the steep magnetic-field dependence of J_c.

In either event these data are consistent with *intrinsic conduction anisotropy* within the crystallites being a significant factor limiting the transport J_c in polycrystalline samples. At grain boundaries between randomly oriented crystallites, there is a situation where the highly conducting Cu-O planes are not in a one-to-one registry. The percolation conductivity will be limited by currents redistributing between the Cu-O planes in the vicinity of each grain boundary. This current-transfer process is limited by the intrinsic weak conduction perpendicular to the Cu-O planes, which could account for at least part of the great difference in J_c between polycrystalline samples and epitaxial thin films[13].

This current-transfer model would suggest that the anisotropy limitation on transport J_c would be significantly greater at polycrystalline grain boundaries than at twin boundaries, since in the case of twinning, there is symmetry across the twin boundary, with a one-to-one correspondence of Cu-O planes on either side. However, in polycrystalline materials, there is a situation such as shown in Fig. 10(b), where many Cu-O planes on the right-hand side of the grain boundary would conduct current into a single Cu-O plane on the left-hand side of the grain boundary. This single plane cannot carry all the current introduced into it and so current is forced to transfer in the weak direction to adjacent Cu-O planes to equalize the current distribution. The geometry is similar to the calculation of current transfer in conventional multifilamentary superconductors,[27] except that here we are considering current transfer between planes on an atomic level as shown in Fig. 10(b), rather than macroscopic filaments.

Different approaches to production of these materials may be necessary for practical bulk applications of $Y_1Ba_2Cu_3O_x$ in light of the anisotropy of the superconducting properties of these materials. In particular, if anisotropy is playing a key role, methods may have to be developed for orienting the crystallites in polycrystalline materials to enhance J_c. This may be accomplished by using a substrate to define a preferred crystal direction in the grains, as was done for the epitaxially grown films of $Y_1Ba_2Cu_3O_x$ described above.[13] More economical techniques suited to bulk high-current conductors might also be possible, such as orienting the grains in the powder state during conductor fabrication.[14]

From the practical standpoint of magnet design, the best orientation would be to have the weak conduction c axis of the $Y_1Ba_2Cu_3O_x$ crystal structure oriented in a direction mutually perpendicular to both the current and field directions. This provides both high critical current and high upper critical field, since the critical field is greatest for magnetic field parallel to the copper-oxygen planes.[12]

VI. CONCLUSIONS

Bulk polycrystalline $Y_1Ba_2Cu_3O_x$ materials are characterized by extreme heterogeneity in their transport properties. This is evidenced by the broad magnetic-field range of the superconducting transition, the sharp decrease in J_c at very low magnetic field, and the significant difference between transport J_c and magnetization J_c. These data also indicate that the transport J_c is characterized by high J_c regions separated by weak-link regions that have a Josephson weak-link conduction behavior.

TEM lattice images showing the mismatch of the Cu-O planes at the grain boundaries, along with recent anisotropy data in epitaxial films and single crystals, indicate that at least part of the limitation on J_c in bulk polycrystalline samples may result from intrinsic conduction anisotropy. The percolation process between randomly oriented grains in bulk samples necessitates a redistribution of currents between the Cu-O planes at grain boundaries. This current-transfer process will be determined by intrinsic weak con-

duction between the Cu-O planes when they are not in a one-to-one registry at the grain boundaries, such as would occur in bulk polycrystalline samples.

Different approaches to production of bulk $Y_1Ba_2Cu_3O_x$ materials may be necessary. If anisotropy is playing a significant role, orienting the grains in the powder state during processing so that the weak conduction c axis is mutually perpendicular to the current and field directions may result in enhanced J_c and H_{c2} in bulk $Y_1Ba_2Cu_3O_x$.

ACKNOWLEDGMENTS

We wish to thank R. B. Goldfarb, J. M. Moreland, R. Radebaugh, L. F. Goodrich, A. F. Clark, R. Langman, D. G. Wirth, J. Sibold, D. R. Clarke, R. Koch, and W. Gallagher for valuable discussions. D. Rule and T. Larson assisted with data analysis. The high magnetic fields needed for this study were obtained using the magnet facilities of the Francis Bitter National Magnet Laboratory. This work was supported at NBS by the Office of Fusion Energy, U.S. Department of Energy, Contract No. DE-AI01-84ER52113 and by a grant from the National Engineering Laboratory and the Director's Office of the National Bureau of Standards. Work at Westinghouse was supported in part by AFOSR Contract No. F49620-85-C-0043 and work at Argonne was supported by DOE/BES Contract No. W-31-109-ENG-38. This paper was presented at the International Cryogenic Materials Conference in St. Charles, Illinois, on 17 June 1987.

[1]J. G. Bednorz and K. A. Müller, Z. Phys. B **64**, 189 (1986).
[2]S. Uchida, H. Takagi, K. Kitazawa, and S. Tanaka, Jpn. J. Appl. Phys. **26** L1 (1987).
[3]C. W. Chu, P. H. Hor, R. L. Meng, L. Gao, Z. J. Huang, and Y. Q. Wang, Phys. Rev. Lett. **58**, 405 (1987).
[4]R. J. Cava, R. B. van Dover, B. Batlogg, and E. A. Rietman, Phys. Rev. Lett. **58**, 408 (1987).
[5]D. W. Capone II, D. G. Hinks, J. D. Jorgensen, and K. Zhang, Appl.
[6]M. K. Wu, J. R. Ashburn, C. J. Torng, P. H. Hor, R. L. Meng, L. Gao, Z. J. Huang, Y. O. Wang, and C. W. Chu, Phys. Rev. Lett. **58**, 908 (1987).
[7]R. J. Cava, B. Batlogg, R. B. van Dover, D. W. Murphy, S. Sunshine, T. Siegrist, J. P. Remeika, E. A. Rietman, S. Zahurak, and G. P. Espinosa, Phys. Rev. Lett. **58**, 1676 (1987).
[8]J. W. Ekin, A. J. Panson, A. I. Braginski, M. A. Janocko, M. Hong, J. Kwo, S. H. Liou, D. W. Capone, II, and B. Flandermeyer, in *High Temperature Superconductors* (Materials Research Society, Pittsburgh, PA, 1987), Vol. EA-11, p. 223.
[9]D. W. Capone, II and B. Flandermeyer, in *High Temperature Superconductors* (Materials Research Society, Pittsburgh, PA, 1987), Vol. EA-11, p. 181.
[10]M. Suenaga, A. Ghosh, T. Asano, R. L. Sabatini, and A. R. Moodenbaugh, in *High Temperature Superconductors* (Materials Research Society, Pittsburgh, PA, 1987), Vol. EA-11, p. 247.
[11]D. C. Larbalestier, M. Daeumling, X. Cai, J. Seutjens, J. McKinnell, D. Hampshire, P. Lee, C. Meingast, T. Willis, H. Muller, R. D. Ray, R. G. Dillenburg, E. E. Hellstrom, and R. Joynt, J. Appl. Phys. **62**, 3308 (1987).
[12]T. R. Dinger, T. K. Worthington, W. J. Gallagher, and R. L. Sandstrom, Phys. Rev. Lett. **58**, 2687 (1987).
[13]P. Chaudhari, R. H. Koch, R. B. Laibowitz, R. R. McGuire, and R. J. Gambino, Phys. Rev. Lett. **58**, 2684 (1987).
[14]J. W. Ekin, Adv. Ceram. Mater. **2**, 586 (1987).
[15]A. J. Panson, A. I. Braginski, J. R. Gavaler, J. K. Hulm, M. A. Janocko, H. C. Pohl, A. M. Stewart, J. Talvacchio, and G. R. Wagner, Phys. Rev. B **35**, 8774 (1987).
[16]S. H. Liou, M. Hong, J. Kwo, and C. L. Chien, AT&T Bell Laboratories (to be published).
[17]J. W. Ekin, Cryogenics **20**, 611 (1980).
[18]D. O. Welch, M. Suenaga, and T. Asano, Phys Rev. B **36**, 2390 (1987).
[19]V. G. Kogan and J. R. Clem, Jpn. J. Appl. Phys. **26**, Suppl. 26-3, 1159 (1987).
[20]C. P. Bean, Phys. Rev. Lett. **8**, 250 (1962).
[21]R. B. Goldfarb, A. F. Clark, A. I. Braginski, and A. J. Panson, Cryogenics **27**, 475 (1987).
[22]J. R. Kirtley, C. C. Tsuei, S. I. Park, C. C. Chi, J. Rozen, and M. W. Shafer, Phys. Rev. B **35** 7216 (1987).
[23]D. C. Larbalestier, M. Daeumling, P. J. Lee, T. F. Kelly, J. Seuntjens, C. Meingast, X. Cai, J. McKinnell, R. D. Ray, R. G. Dillenburg, and E. E. Hellstrom, Cryogenics **27**, 411 (1987).
[24]T. P. Orlando, K. A. Delin, S. Foner, E. J. McNiff, Jr., J. M. Tarascon, L. H. Greene, W. R. McKinnon, and G. W. Hull, Phys. Rev. B **36**, 2394 (1987).
[25]T. Y. Hsiang and D. K. Finnemore, Phys. Rev. B **22**, 154 (1980).
[26]F. M. Mueller, J. Met. **39**, 6 (1987); and J. Yu, S. Massidda, A. J. Freeman, and D. D. Koelling, Phys. Lett. A **122**, 203 (1987).
[27]J. W. Ekin, J. Appl. Phys. **49**, 3406 (1978).